

Evaluation of Dose in Gamma-Ray with White Light-Sensitive Phosphor Material in low Temperature

P. Rubalajyothi, A. Rajendran*

Department of Physics, Nehru Memorial College (Autonomous) and affiliated to Bharathidasan University, Puthanampatti, Tiruchirappalli-07, Tamilnadu, India

*Corresponding Author: neelrajnmc@gmail.com

Article Info

Volume 82

Page Number: 8137 - 8150

Publication Issue:

January-February 2020

Abstract

Dysprosium doped Barium Calcium Sulphate polycrystalline has been used to perform thermoluminescence studies at different heating rates from lower to higher range of 10 Gy to 2000 Gy. Thermoluminescence spectra showed almost equal peaks and most of the major intensity high points have extreme temperatures of 110, 114, 127 and 125 K exposure. These materials are very effective and sensitive in low dose level response with superb linearity. Using the glow curve fitting to calculate the geometry factor, energy values are observed at all dose levels. Catch cross-segments of each dimension are additionally assessed by utilizing the obtained energy esteems. Additionally, the warming rate conditions of the obtained high points were also examined. It is demonstrated that while the dose level increased, the peak intensity also increased by about 10 Gy to 700 Gy and it reached the maximum dose. Because after 700 Gy doses level, to expose the gamma radiation, the glow curves are splitting further studies were conducted to reduce the voltage value to 800 mV using up to 2000 Gy.

Article History

Article Received: 18 May 2019

Revised: 14 July 2019

Accepted: 22 December 2019

Publication: 05 February 2020

Keywords: - Low Temperature with High Heating Rates; T_{max} ; Thermoluminescence; Peak Intensity, linear response.

I. Introduction

The (II) and (VI) group contain alkali earth metals having (+2) oxidation state like in the compound $BaCaSO_4$ having a layered structure, that is found useful for the generation of optic-electro-chemicals in red, yellow and blue light-emitting diode materials [1– 4]. Specialists have researched the electrical and optical properties of these kinds of valuable shingles to learn about conceivable utilization in innovation.

Phosphors were assumed as essential in the iridescence of white light-radiating diode

(Drove). To get white light via ordinary techniques, the RGB technique and phosphor strategy is usually used. The RGB technique includes separate imperfections for producing red,

green and blue light; henceforth this strategy is confusing and is expensive in structure gadgets [5– 6]. The phosphor strategy obtains white photons by coordinating InGaN Drove chip with yellow-emitting $Y_3Al_5O_{12}: Ce^{3+}$ (YAG: Ce^{3+}) phosphor. By this strategy, cool white light is created by mealy red discharge parts in a yellow phosphor [7– 10]. Avoiding these issues, cool white light can be created by utilizing a solitary emitting focus with a yellow phosphor having a high shading interpretation list and low correlated shading temperature. Because of its grand glow properties, rare earth components have assumed a noteworthy role in present daylighting. High shading excellence can be accomplished by f– f electronic transfer in rare earth particles [11– 14]. As an essential individual from the infrequent earth particles, the trivalent europium particle

(Eu³⁺) is an amazing red-emanating initiating specialist because of $^5D_0 \rightarrow ^7F_J$ ($J = 0, 1, 2, 3, 4$).

When an alkali earth's metal or phosphor with profound traps is presented to gamma radiation for some time at low temperatures, it integrates energy from the radiation and the intense device. At that point when the temperature of the material is raised, it demonstrates an expanded glow called thermally stimulated luminescence (TSL), because of the recombination of the thermally reactive electrons from the profound traps where the vitality is changed over to radiance and discharged light as noticeable. This phenomenon is known as Thermoluminescence (TL) [15]. The warmth just goes about as a stimulant through the ionizing radiation that assumes the job of an energizing operator. In the process of illuminating a material with beams, β -beams, UV-beams, χ -beams, or γ -beams, some portion of the light vitality is utilized to exchange electrons to traps [16].

A portion of these collected electrons themselves at a intensity (E) beneath the conduction band. The trap levels or focuses assume a huge carrier amount of energy from the ground state to excited state in vitality storing for determined photoluminescent and thermoluminescent phosphors. This radiation vitality is put-away as the collected electrons are discharged by raising the temperature of the material and the discharged vitality is changed over to iridescence. This infectious procedure pursued by the arrival of put-away vitality in thermoluminescent materials is broadly used in radiology, for example in ionizing radiation dosimeter. Every single bright material may have a base edge temperature for the arrival of recently put away energy, yet many have a base activating temperature under normal temperatures [17].

To get data about the radiance procedure of phosphors and to apply them in different fields, the information of imperfections or traps and their area in the band hole of these materials is

dynamic. TL estimation is an essential and advantageous strategy for research and for giving data concerning the idea of traps and communicable dimensions in residues. The glow curve, which is an interpretation of the temperature reliance of the release power, is a decent way to quantify the snare profundity [18]. During TL estimation, the illuminating source is cut off and thermally energized glow is recorded when the temperature is increased gradually. The different parameters of the catching procedure like initiation vitality (E), the measure of the snare, infectious frequency, and so forth, are then concluded by breaking down the shape and position of the obtained TL glow curve [19]. Thermoluminescence (TL) is an outstanding phenomenon, which is brought about by the thermally-assisted light initiated electrons from the traps of the material. The TL material can give profitable data about the natural imperfection of materials and the burning beam to which the material was exposed. Consequently, it is broadly used in the fields of deformity contemplating, dating in paleontology, illumination discovery, etc.

In this TL glow curve shape factor ≈ 0.52 corresponds to second-order kinetic energy. The initiation vitality and frequency factors are estimated to be in the range of 0.6 to 1.2 eV and $5.07 \pm 0.05 \times 10^6$ to $3.09 \pm 0.01 \times 10^{15}$ respectively [20-27]. The present paper reports the examinations of TL properties of Dy³⁺ doped Ba_{1-x}Ca_xSO₄ at dosages higher than 10 Gy up to 2 KGy, i.e. above the ostensible interest level (10 Gy–700 Gy) of TLD material. TL glow curves in different mole percentages of doped Dy³⁺ material due to adjustments in TL supra linearity at high dose irradiation.

II. Materials and methods

Ba_{1-x}Ca_xSO₄: Dy³⁺ was doped at different mol % to the stoichiometric ratio to adding the distilled water. Crude materials were prepared in the beaker and transferred to a quartz tube for 30

minutes – 45 minutes of stirring to paste level and then dried at 440 °C for 10mins. The collected powder was fed to an agate motor to be made into a fine powder. The Dy³⁺ doped Ba_{1-x}Ca_xSO₄ powder's stage arrangement was confirmed by powder x-beam diffraction strategy which utilizes an 'X' Perky Expert PANalytical diffractometer having Cu-K α radiation ($\lambda = 1.54060\text{\AA}$) as a source and which works at 40 kV and 30 MA. The example was examined in 2 θ extending from 10° to 80° for 2s in progression check mode.

For the assurance of precious stone structure, the samples were examined by x-beam diffraction. For Thermoluminescence equipment, nucleonic TLD framework manual TL peruser which is a PC driven, physically worked, instruments for Thermoluminescence dosimeters estimation was utilized. The TL gleam bends were recorded with a typical setup consisting of a little metal plate warmed specifically by utilizing a temperature developer, photomultiplier, dc speaker and a plant volt recorder. Tests were presented to X-beam and gamma beams from a cobalt-60 source at room temperature. After the presentation, TL shine curves were recorded for 10 mg of an analysis, each time at a warming rate 5°Cs⁻¹ for the equivalent and diverse portion. For correlation, glow curves were additionally recorded.

2.1. Characterization

PANALYTICAL X' Pert Genius X-beam diffractometer was utilized for the investigation of phase with structure identification. The oxidation condition was checked by X-beam photoelectron spectroscopy (XPS) having Source Gun A = X-Ray 014 400um - FG ON (400 μm) mode. The facilities were available at the Indira Gandhi atomic research facility in Kalpakkam. The TLD reader (5p-400) nucleonic system and use the gamma-ray chamber.

III.III. Results and Discussion

3.1 Barium Calcium Sulphate spectra for XPS studies

The photoelectron spectra was collected on Source Gun A = X-Ray 014 400um - FG ON (400 μm). The examples spectra were procured at room temperature by utilizing a monochromatic Alka (1486 eV) X-ray radiation. XPS Investigation of BaCaSO₄:Dy³⁺ Fig.1. Demonstrate the study spectra of the powders under investigation. Recording of such spectra directed in high affectability mode makes it possible to consider the primary lines of all components exhibited in the surface layer of the material. All the peaks are identified by the electronic dimensions of dysprosium, barium, calcium, sulfur, and oxygen contained in the arrangement of the exceptional earth soluble base materials under investigation. The firmly expanded barium peak (represented as a doublet of Ba 3d_{5/2} –Ba 3d_{3/2}) in the spectra of enacted tests affirm the redistribution of the components between the volume and the surface. This represents the aftereffect of synthetic corruption on the surface affected by a situation. The examination of the Ba 3d spectra shows barium carbonate (line Ba 3d_{5/2} at 781.48 eV and Ba 3d_{3/2} 796 eV) and there is BaSO₄ (line Ba 3d_{5/2} at ~782 eV) outside the examples [28]. The coupling vitality of calcium (Ca 2p), which squares with 349 eV proposes that calcium is on the second phase of oxidation (Ca²⁺) and is present in all likelihood as CaHPO₄ and additionally Ca₃(PO₄)₂ [29]. On the S_{2p} crest, the ionized have been emphatically oxidized with an S_{2p} commitment and currently show up at around 170 eV restricting vitality and thus verifying the nearness of sulfate table.1. The sulfur 2p standard can be studied by parts having a similar combined Gaussian line-shape and having FWHM of 2.79 eV.

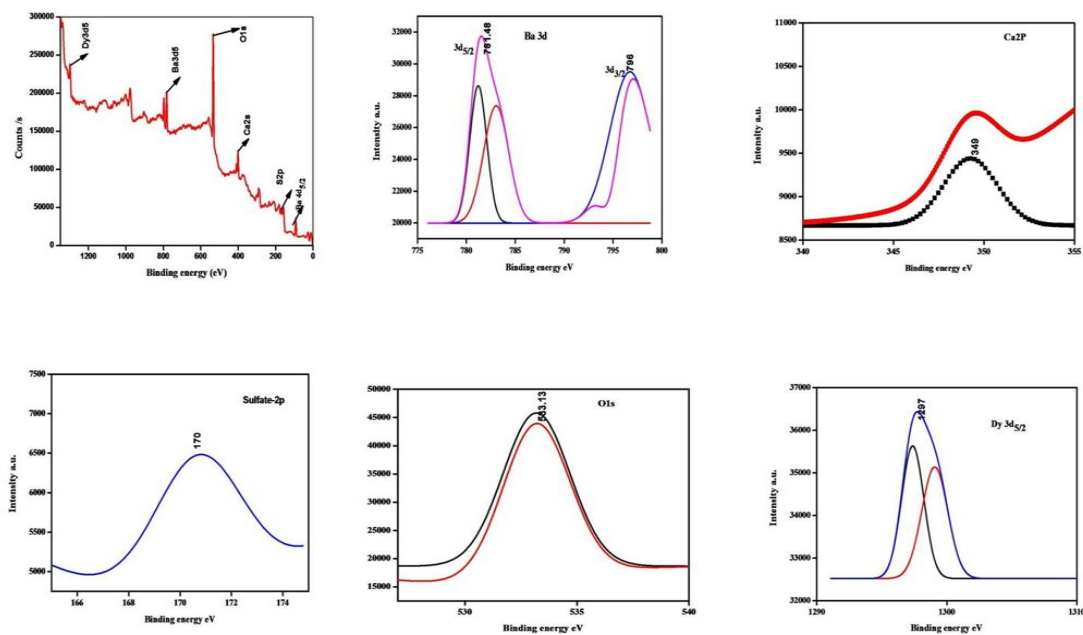


Fig. 1. XPS survey for dysprosium doped barium calcium Sulphate with curve fitting for binding energy

Sulfur 2p restricting the vitality gives a delicate proportion of the electronic character an atom oxidized in sulfur molecules or ions and whose shapes are sincerely fixed, for example, sulfoxides - (166 eV), sulfones - (168 eV) and sulfonic Corrosive/sulfate - (169 eV). From the results of deconvolution in the O_{1s} XPS spectra, the O_{1s} peaks like 533.1±0.1 eV is assigned to oxide. Thus, in the Dysprosium 3d_{5/2} range from the (Fig.1). The low values at 1294.5 eV corresponding to, the fundamental stage with high values at 1296.4 eV corresponding to Dy₂O₃ [30].

Name	Peak BE	FWHM eV
Ba3d _{5/2,3/2}	781.48,796	3.35
Ca2p	349	1.73
S2p	170	2.79
O1s	533.13	3.44
Dy3d ₅	1297	5.84

Table.1. XPS survey for dysprosium doped barium calcium Sulphate with binding energy

3.2 TL studies:

Modernized glow bend de-convolution (CGCD) is an incredible asset in the examination of sparkle bends. It comprises essential capacities like second-order kinetics [31], the general request energy [32] and the technique of Levenberg–Marquardt (LM) [33] which is a daily practice in the least-squares strategy for non-straight functions.

3.2.1. Thermoluminescence Studies of Ba_{1-x}Ca_xSO₄: Dy³⁺ Glow Curves

3.2.1.1. Study of the kinetic parameters

The TL shine bend demonstrates the snare nearness in that material and gives the data regarding the vitality consumed by the substance among illumination. From that, Fig. 2 to analyzing the values was geometry factors and order of kinetics to use Chen’s shape peak method to find the second-order kinetics values. Using the second-order formulas was analyzing the activation energy and frequency factor.

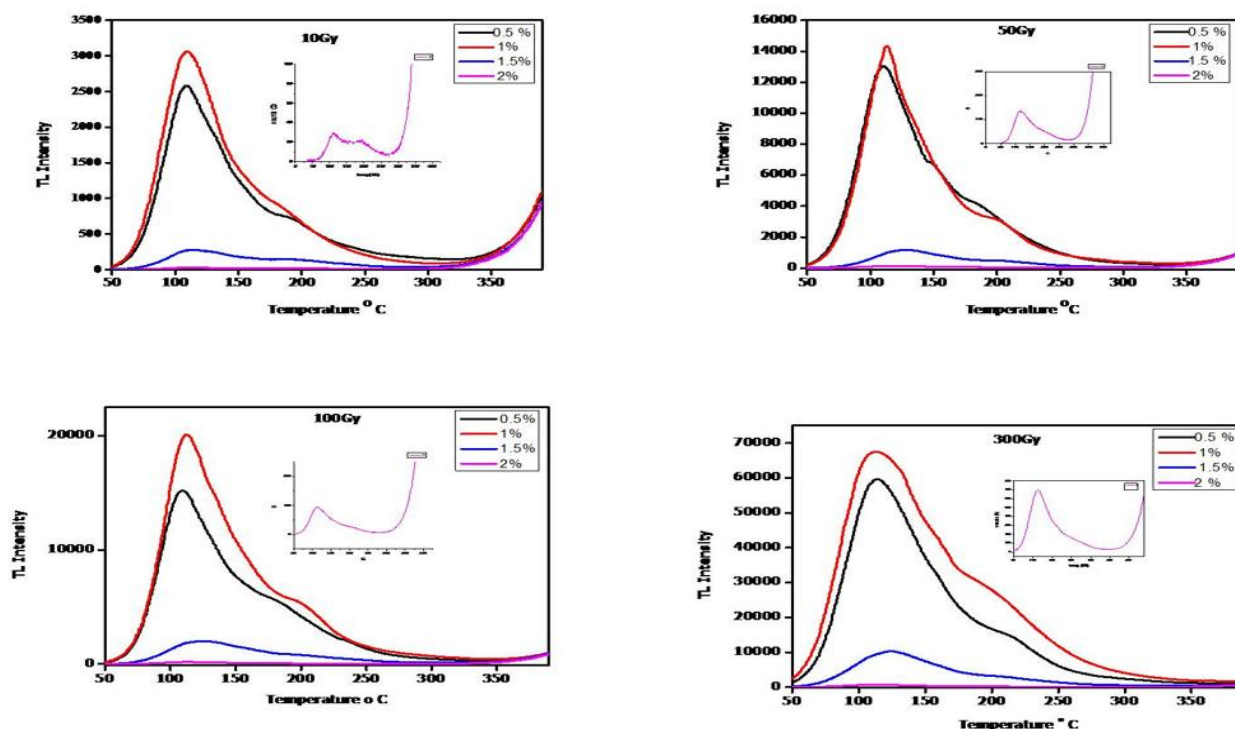


Fig. 2. Thermoluminescence studies to using the gamma rays exposure to low Dose for 10 Gy to 300 Gy for doping dysprosium

Fig.2. Shows gamma-ray beam exposure from 10 Gy to 300 Gy for the time duration of one minute - 10 minutes. TL energy curve for (Ba, Ca) SO₄: Dy³⁺ phosphor was recorded with a gamma chamber presentation of 10 Gy to 2 KGy (2 min

up to 1 hr) at a heating rate of 5k/s. The kinetics of parameters, activation energy, and frequency factor were calculated using Chen's empirical formula. The kinetic parameter of (Ba, Ca) SO₄: Dy³⁺ phosphor are recorded in table 2.

Dose rate (Gy)	Materials/ratio Ba _{1-x} Ca _x SO ₄ :Dy ³⁺	Symmetry factor (μg)	Order of kinetics (b)
10 Gy	Ba _{0.97} Ca _{0.03} SO ₄ :Dy _{0.5}	0.57	0.57±0.04
	Ba _{0.95} Ca _{0.05} SO ₄ :Dy ₁	0.62	0.62±0.05
	Ba _{0.93} Ca _{0.07} SO ₄ :Dy _{1.5}	0.64	0.64±0.09
	Ba _{0.91} Ca _{0.09} SO ₄ :Dy ₂	0.64	0.64±0.04
Total			0.61±0.05
50 GY	Ba _{0.97} Ca _{0.03} SO ₄ :Dy _{0.5}	0.63	0.63±0.09
	Ba _{0.95} Ca _{0.05} SO ₄ :Dy ₁	0.57	0.57±0.02
	Ba _{0.93} Ca _{0.07} SO ₄ :Dy _{1.5}	0.61	0.61±0.06
	Ba _{0.91} Ca _{0.09} SO ₄ :Dy ₂	0.65	0.65±0.04
Total			0.61±0.05
100 Gy	Ba _{0.97} Ca _{0.03} SO ₄ :Dy _{0.5}	0.61	0.61±0.08
	Ba _{0.95} Ca _{0.05} SO ₄ :Dy ₁	0.64	0.64±0.05
	Ba _{0.93} Ca _{0.07} SO ₄ :Dy _{1.5}	0.61	0.61±0.04
	Ba _{0.91} Ca _{0.09} SO ₄ :Dy ₂	0.60	0.60±0.07
Total			0.61±0.05
300 Gy	Ba _{0.97} Ca _{0.03} SO ₄ :Dy _{0.5}	0.62	0.62±0.06
	Ba _{0.95} Ca _{0.05} SO ₄ :Dy ₁	0.61	0.61±0.06

	Ba _{0.93} Ca _{0.07} SO ₄ :Dy _{1.5}	0.56	0.56±0.06
	Ba _{0.91} Ca _{0.09} SO ₄ :Dy ₂	0.58	0.56±0.03
		Total	0.58±0.05

Table. 2. Analyzing the geometric factor values to finding the order of kinetics From Thermoluminescence material in gamma ray from 10 Gy to 300 Gy

Dosimetry conditions such as each and every peak are very sensitive and high response with a single glow curve. In this, the material is observed and analyzed with up to 700 Gy with 900 mV TL peak intensity. Most of the rare earth materials have high peak intensity at the same dose level at high temperature due to an increase in gamma-ray exposure by slightly different mol percentage in T_{max} temperature. The peaks are clearly present in the visible region [34, 35]. By the following equation 1, the symmetry values are evaluated.

$$\mu_g = \delta/\omega \quad (1)$$

Here, by using Chen's peak the symmetry factor and order of kinetics are analyzed. Here, most of the mol percentage doped dysprosium materials seem to be following second-order kinetics. After that by using the second-order Chen's shape peak method, activation energy, and frequency factor values are calculated. The activation energy and frequency factor values are dependent only on temperature. Here T₁, T₂, and T_m are the lowest, highest and maximum temperature respectively. In that material, the pinnacles are available in first and second-order kinetic energy. Consequently, it implies that Ba_{1-x}Ca_xSO₄:Dy³⁺ shows the normal qualities at 0.57

which is close to near Chen's second-order kinetic energy [36]. The initiations of vitality and recurrence factor esteems are recorded in table.2.

The TL glow curve was recorded for 10 mg of samples at a linear heating rate of 5°Cs⁻¹ for the same dose. When there is an increase in the concentration of Dy³⁺, there is an increase in the peak intensity which depends on temperature with sensitivity. To irradiate the gamma chamber to expose low dose to high dose rays for passing the phosphor materials with dependence at time duration up to a maximum one hour. To increase the dopant's mol percentage depending on the high response in Dysprosium, it was observed that with expanding fixation dopants of Dysprosium one-mole percentage to exposing gamma rays, the outcome will be very effective and sensitive with the high response in that material. As per this model, the discovery of the recombination of lumini/catching focuses happens inside the tracks at a low illumination portion.

A good dosimeter characteristic such as a single glow curve with just one peak at a low dose and high response of TL sensitivity is seen. According to this, above said conditions are satisfied in our material and its powder shows good TL sensitivity even at the low dose of gamma-ray. The gamma-ray increased by up to

700 Gy to reach maximum temperature and after that, the intensity peak decreased depending on dose level. The low dose in the range of 10 Gy to

700 Gy is useful for radiation dosimeters and clinical processes.

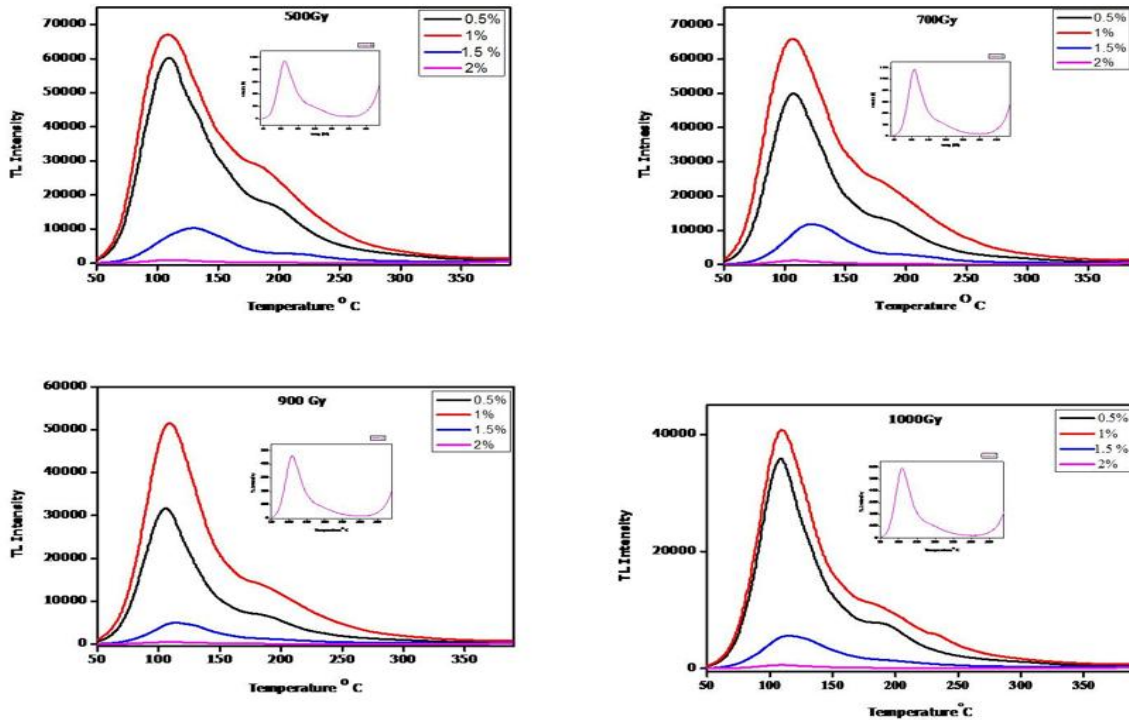


Fig. 3. Thermoluminescence studies to using the gamma rays exposure to high Dose for 500 Gy to 1000 Gy

Fig. 3, 4. Exposes the gamma rays with a high dose of 900 Gy to 2 Kgy, following Chen's shape peak method to obey the second-order of kinetics in the table (3).

$$E_{\tau} = \frac{1.81 KT^2 M}{\tau} - 2(2KTm) \quad (2)$$

$$E_{\delta} = 1.71 \frac{KT^2 M}{\delta} \quad (3)$$

$$E_{\omega} = 3.54 \frac{KT^2 M}{\omega} - 2KTm \quad (4)$$

$$S = \frac{\beta E}{KT^2 M(1 + \frac{2KTm}{E})} \exp E \frac{E}{KTm} \quad (5)$$

Eq. (2, 3, 4, and 5) is Chen's shape peak method second-order active articulation of a solitary glow peak. I (T) is the intensity as a function of temperature, β is the constant heating rate and Tm is the temperature, k is Boltzmann constant $8.617 \times 10^{-5} \text{ eV K}^{-1}$, T is the absolute temperature, S is the frequency factor and E is the trap depth or activation energy, the energy needed to release an electron from the trap into the conduction band.

Dose rate (Gy)	Materials / ratio ($\text{Ba}_{1-x}\text{Ca}_x\text{SO}_4:\text{Dy}^{3+}$)	Symmetry factor (μg)	Order of Kinetics (b)
500Gy	$\text{Ba}_{0.97}\text{Ca}_{0.03}\text{SO}_4:\text{Dy}_{0.5}$	0.58	0.58 ± 0.06

	Ba _{0.95} Ca _{0.05} SO ₄ :Dy ₁	0.59	0.59±0.09
	Ba _{0.93} Ca _{0.07} SO ₄ :Dy _{1.5}	0.48	0.48±0.07
	Ba _{0.91} Ca _{0.09} SO ₄ :Dy ₂	0.58	0.58±0.05
	Total		0.55±0.05
700Gy	Ba _{0.97} Ca _{0.03} SO ₄ :Dy _{0.5}	0.58	0.58±0.01
	Ba _{0.95} Ca _{0.05} SO ₄ :Dy ₁	0.56	0.56±0.06
	Ba _{0.93} Ca _{0.07} SO ₄ :Dy _{1.5}	0.55	0.55±0.07
	Ba _{0.91} Ca _{0.09} SO ₄ :Dy ₂	0.58	0.58±0.09
	Total		0.56±0.05
900Gy	Ba _{0.97} Ca _{0.03} SO ₄ :Dy _{0.5}	0.58	0.58±0.01
	Ba _{0.95} Ca _{0.05} SO ₄ :Dy ₁	0.55	0.55±0.03
	Ba _{0.93} Ca _{0.07} SO ₄ :Dy _{1.5}	0.6	0.6±0.04
	Ba _{0.91} Ca _{0.09} SO ₄ :Dy ₂	0.56	0.56±0.02
	Total		0.57±0.05
1 KGy	Ba _{0.97} Ca _{0.03} SO ₄ :Dy _{0.5}	0.57	0.57±0.04
	Ba _{0.95} Ca _{0.05} SO ₄ :Dy ₁	0.57	0.57±0.04
	Ba _{0.93} Ca _{0.07} SO ₄ :Dy _{1.5}	0.61	0.61±0.07
	Ba _{0.91} Ca _{0.09} SO ₄ :Dy ₂	0.59	0.59±0.09
	Total		0.58±0.05
2 KGy	Ba _{0.97} Ca _{0.03} SO ₄ :Dy _{0.5}	0.56	0.56±0.06
	Ba _{0.95} Ca _{0.05} SO ₄ :Dy ₁	0.54	0.54±0.01
	Ba _{0.93} Ca _{0.07} SO ₄ :Dy _{1.5}	0.54	0.54±0.06
	Ba _{0.91} Ca _{0.09} SO ₄ :Dy ₂	0.51	0.51±0.02
	Total		0.53±0.05

Table. 3. Analyzing the geometric factor values to finding the order of kinetics from Thermoluminescence material in gamma ray from 500 Gy to 2 KGy

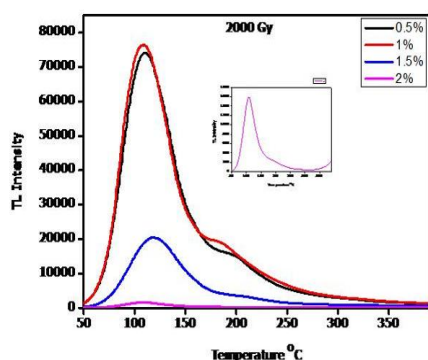


Fig. 4. Thermoluminescence studies to using the gamma rays exposure to high Dose with supralinearity response for 2000 Gy doping dysprosium

3.2.2. TL response

The phosphor materials were exposing the gamma-ray chamber to low level to high-level dosage with a maximum one hour [36-42]. A TL reaction bend of Ba_{1-x}Ca_xSO₄ doped with Dy³⁺ phosphor presented at various dosages of gamma beams is given in Fig. 1, 2, 3 respectively. The peak statues are utilized for estimating the TL forces. This range is a decent outcome for a material that can be utilized as a dosimeter.in that materials were different mole percentages with the dopant. The ratio of one-mole percentage composition of the material is very effective with a linear response in low to high dose level in the table. 1, 2. The calculated activation energy

with frequency factor values is given in the table.

4.

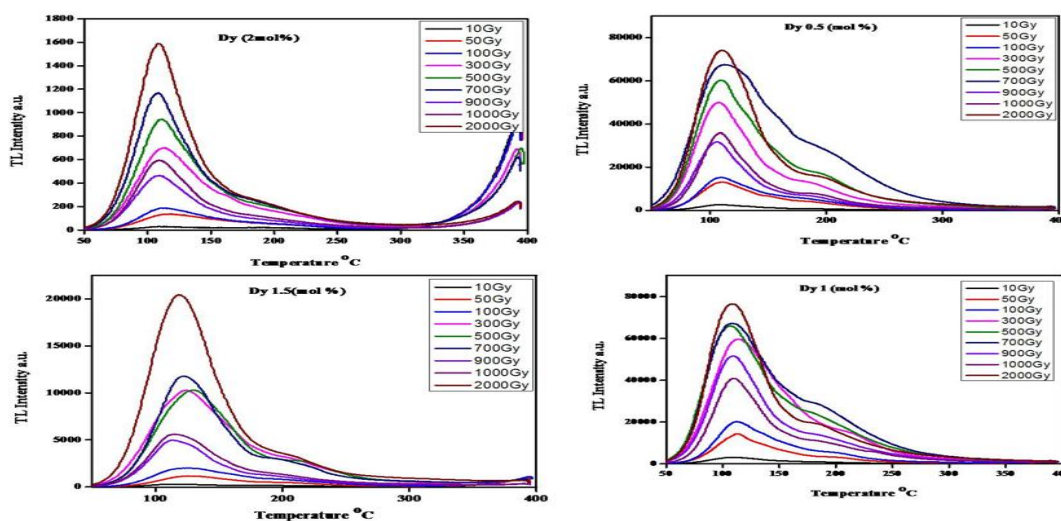


Fig. 5. Thermoluminescence glow curve measured doped dysprosium with Different ratio and different dose in gamma chamber from 10 Gy to 2000 Gy

According to that from Fig. 5. 10 Gy to 700 Gy, the peak intensity will increase gradually to the maximum temperature and it will be returned to high dose with the low-intensity peak value of $\approx 40\%$ to reduce in our materials which means the critical dose range is between 900 Gy-1000 Gy the peak will be lost. Due to exposure to the high dose level at 900 Gy with 900 mV, the maximum peaks should be splitting or damage

due to particle size. I have continued the further process of reducing the voltage level to 800 mV up to 2 KGy. After that to change the temperature and to expose the 2 KGy doses, it suddenly gave high-intensity peaks with supra-linearity. In table. 3 by using Chen's shape peak method to analyze the second-order kinetic parameters, activation energy, and frequency factor are given

Dose rate(Gy)	Materials /ratio	τ	ω	δ	E_{τ}	E_{ω}	E_{δ}	E_{avg} (ev)	Frequency factors (S^{-1})
10 Gy	$Ba_{0.97}Ca_{0.03}SO_4:Dy_{0.5}$	20	47	27	1	0.8	0.79	0.86 ± 0.03	$8.11 \pm 0.05 \times 10^{10}$
	$Ba_{0.95}Ca_{0.05}SO_4:Dy_1$	18	48	30	1.13	0.86	0.7	0.89 ± 0.06	$1.81 \pm 0.02 \times 10^{11}$
	$Ba_{0.93}Ca_{0.07}SO_4:Dy_{1.5}$	19	53	34	1	0.79	0.64	0.81 ± 0.05	$1.24 \pm 0.03 \times 10^{10}$
	$Ba_{0.91}Ca_{0.09}SO_4:Dy_2$	13	37	24	1.16	1.21	0.9	1.2 ± 0.03	$3.09 \pm 0.01 \times 10^{15}$
50 Gy	$Ba_{0.97}Ca_{0.03}SO_4:Dy_{0.5}$	17	47	30	1.2	0.9	0.7	0.92 ± 0.06	$4.67 \pm 0.08 \times 10^{11}$
	$Ba_{0.95}Ca_{0.05}SO_4:Dy_1$	18	42	24	1.15	1	0.9	1.02 ± 0.05	$7.67 \pm 0.04 \times 10^{12}$
	$Ba_{0.93}Ca_{0.07}SO_4:Dy_{1.5}$	23	59	36	0.94	0.76	0.65	0.78 ± 0.03	$1.8 \pm 0.01 \times 10^9$
	$Ba_{0.91}Ca_{0.09}SO_4:Dy_2$	24	70	46	0.85	0.59	0.48	0.6 ± 0.04	$1.4 \pm 0.05 \times 10^7$
100 Gy	$Ba_{0.97}Ca_{0.03}SO_4:Dy_{0.5}$	20	52	32	1.01	0.79	0.67	0.82 ± 0.03	$2.14 \pm 0.05 \times 10^{10}$
	$Ba_{0.95}Ca_{0.05}SO_4:Dy_1$	23	65	23	0.87	0.63	0.52	0.67 ± 0.03	$1.28 \pm 0.01 \times 10^8$
	$Ba_{0.93}Ca_{0.07}SO_4:Dy_{1.5}$	29	76	47	0.7	0.6	0.5	0.58 ± 0.06	$5.07 \pm 0.05 \times 10^6$
	$Ba_{0.91}Ca_{0.09}SO_4:Dy_2$	21	53	32	0.97	0.79	0.69	0.81 ± 0.06	$1.24 \pm 0.06 \times 10^{10}$
300 Gy	$Ba_{0.97}Ca_{0.03}SO_4:Dy_{0.5}$	25	67	42	0.79	0.61	0.52	0.64 ± 0.05	$6.19 \pm 0.02 \times 10^7$

	Ba _{0.95} Ca _{0.05} SO ₄ :Dy ₁	23	60	37	0.9	0.69	0.59	0.72±0.07	7.47±0.05x10 ⁸
	Ba _{0.93} Ca _{0.07} SO ₄ :Dy _{1.5}	26	60	34	0.8	0.73	0.7	0.76±0.03	1.14±0.05x10 ⁹
	Ba _{0.91} Ca _{0.09} SO ₄ :Dy ₂	24	55	31	0.84	0.76	0.71	0.77±0.03	3.55±0.05x10 ⁹
500 Gy	Ba _{0.97} Ca _{0.03} SO ₄ :Dy _{0.5}	24	58	34	0.82	0.7	0.63	0.71±0.06	6.65±0.05x10 ⁸
	Ba _{0.95} Ca _{0.05} SO ₄ :Dy ₁	22	54	32	0.9	0.76	0.67	0.77±0.06	3.75±0.05x10 ⁹
	Ba _{0.93} Ca _{0.07} SO ₄ :Dy _{1.5}	32	62	30	0.66	0.73	0.8	0.71±0.03	1.65±0.04x10 ⁸
	Ba _{0.91} Ca _{0.09} SO ₄ :Dy ₂	22	53	31	0.9	0.8	0.7	0.79±0.06	7.75±0.04x10 ⁹
700 Gy	Ba _{0.97} Ca _{0.03} SO ₄ :Dy _{0.5}	26	63	37	0.73	0.63	0.57	0.64±0.03	7.35±0.05x10 ⁷
	Ba _{0.95} Ca _{0.05} SO ₄ :Dy ₁	21	52	31	0.94	0.78	0.68	0.8±0.05	1.16±0.04x10 ¹⁰
	Ba _{0.93} Ca _{0.07} SO ₄ :Dy _{1.5}	25	56	31	0.84	0.78	0.74	0.78±0.06	2.26±0.06x10 ⁹
	Ba _{0.91} Ca _{0.09} SO ₄ :Dy ₂	18	43	25	1.12	0.96	0.86	0.97±0.06	2.44±0.08x10 ¹²
900 Gy	Ba _{0.97} Ca _{0.03} SO ₄ :Dy _{0.5}	21	50	29	0.94	0.82	0.73	0.83±0.03	2.89±0.07x10 ¹⁰
	Ba _{0.95} Ca _{0.05} SO ₄ :Dy ₁	17	38	21	1.18	1.08	1	1.08±0.06	9.28±0.03x10 ¹³
	Ba _{0.93} Ca _{0.07} SO ₄ :Dy _{1.5}	20	50	30	1.03	0.84	0.74	0.87±0.03	8.00±0.02x10 ¹⁰
	Ba _{0.91} Ca _{0.09} SO ₄ :Dy ₂	20	46	26	1	0.9	0.82	0.9±0.06	2.51±0.01x10 ¹¹
1 KGy	Ba _{0.97} Ca _{0.03} SO ₄ :Dy _{0.5}	20	47	27	1.01	0.95	0.8	0.87±0.05	8.87±0.01x10 ¹⁰
	Ba _{0.95} Ca _{0.05} SO ₄ :Dy ₁	18	42	24	1.12	0.98	0.9	0.99±0.06	4.58±0.06x10 ¹²
	Ba _{0.93} Ca _{0.07} SO ₄ :Dy _{1.5}	26	68	42	0.77	0.61	0.53	0.63±0.06	3.12±0.09x10 ⁷
	Ba _{0.91} Ca _{0.09} SO ₄ :Dy ₂	22	54	32	0.9	0.75	0.7	0.77±0.03	4.07±0.05x10 ⁹
2 KGy	Ba _{0.97} Ca _{0.03} SO ₄ :Dy _{0.5}	20	51	31	1	0.8	0.7	0.83±0.02	2.98±0.09x10 ¹⁰
	Ba _{0.95} Ca _{0.05} SO ₄ :Dy ₁	23	51	28	0.86	0.81	0.77	0.81±0.03	1.34±0.08x10 ¹⁰
	Ba _{0.93} Ca _{0.07} SO ₄ :Dy _{1.5}	22	48	26	0.94	0.9	0.86	0.9±0.07	1.45±0.04x10 ¹¹
	Ba _{0.91} Ca _{0.09} SO ₄ :Dy ₂	19	39	20	1.06	1.07	1.07	1.06±0.06	3.86±0.07x10 ¹³

Table. 4. Chen's shape peak method to analyzing second order kinetics Parameter, Calculate the activation energy and frequency factor

The measure of rare glow curve of Dy³⁺ doped Ba_{1-x}Ca_xSO₄ at a warming rate of 5°C /s is given in Fig. 5. In which it's observed that the states of the gleam bends have not significantly changed the inspiration of increasing the dose within the scope of high dose irradiation in TL material. to exposing the gamma-ray up to 700 Gy the peaks are gradually increased. The force of glow bends diminishes to ≈ 40% of its unique esteem after illumination with 2 KGy. As observed in Fig. 4. All the mol percentage of dysprosium doped Ba_{1-x}Ca_xSO₄ same dose with different dysprosium mol percentage values are compared. Expanding the dose level increases as well as increased in the response level. All the

different ratio composition of the materials was a good response with linear response. I am sure that the dysprosium material was the very effective and highly radioactive response; it is used in the dosimetry process in the medical field [43]. As seen in Fig. 4. The assessment glow curve of different mol% of Dy³⁺ doped Ba_{1-x}Ca_xSO₄ consists of one peak, which is built by TLD reader software application initially from the TL standard collected by TLD peruser. A glow curve (single peak) is seen with the most extreme force at 127 °C.

All glow curves are dissected by the TLD reader 5p-400 software programming to acquire the shine crests (second-order) and assess its

dynamic parameters and the obtained outcomes that are given in Fig. 6.

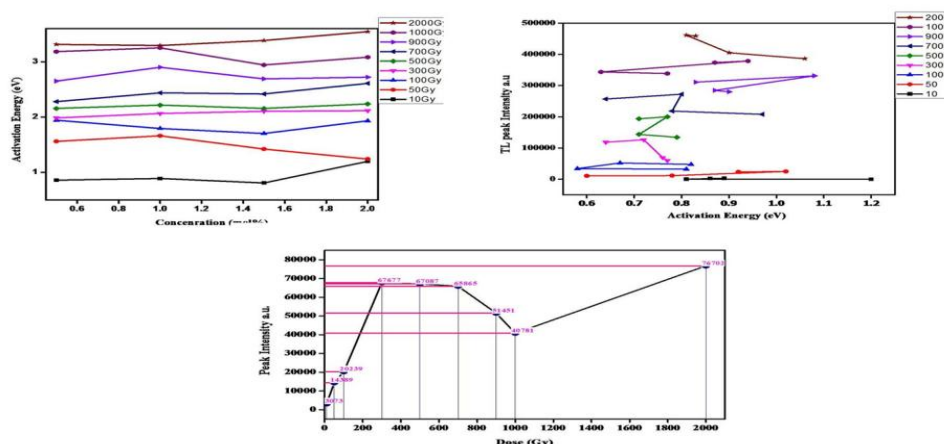


Fig. 6. Comparing the studies of activation energy, concentrations of dysprosium, High dose level with gamma irradiation

It can be noticed that the concentration ratio increased due to increasing activation energy. The activation energy increase, as well as the frequency factor values, increased. Fig. 5. Display or depict with expanding energy versus T_{max} , which means activation energy values are increased with dependence on T_{max} intensity. The outcomes demonstrated that a large amount of enactment vitality E needs a higher temperature to discharge electrons. At that dose level, increasing up to 10 Gy to 700 Gy, the glow curves are gradually increased with linear response.

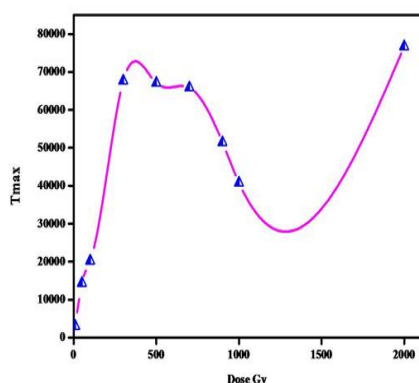


Fig. 7. The linearity response of the Thermoluminescence studies to using the Gamma rays exposure 10 Gy to 2000 Gy $Ba_{1-x}Ca_xSO_4:Dy^{3+}$

In Fig. 7. A huge decline in the highest temperature of the gleaming curve ($127\text{ }^\circ\text{C} - 109\text{ }^\circ\text{C}$) is seen as the high dose increase from 10 Gy to 2 Kgy. The time taken to achieve its most extreme shine peak was additionally diminished from 10 Gy to 700 Gy with an expanded portion. As the portion expands, the width of the shine bends also increases. An increase in dose rate due to the glow curve increase is dependent on the high gamma-ray exposure dosage. The major peak, which is also connected to the pinnacle area, shows the number of free electrons that travel from the devices to the glow focus. In particular, in that gamma-ray exposure of 900 mV with 700 Gy showed extremely high response in our outcome results. At that point, further increment in portion would result in a significant decrease in the glow bend territory by $\approx 40\%$ Fig. 6.

Generally, in our studies, a further increase in percentage, after the highest $f(D)$, causes a critical decline in $f(D)$. This is called the basic portion limit of this TL material. After the basic portion limit is accomplished, the critical decline in pinnacle stature happens by $\approx 40\%$. The width of the glow bends likewise increases when the portion is expanding above 700 Gy to observe the high peak intensity. To expose the high

amount of radiation dose level, the glow curves are splitting. So I am sure that the particles should be damaged or to reduce the size. Because to using the high heating rate at 5°C/S. To refer the authors are told that the particle size is up to 58 nm to 78 nm. But I have to use the combustion method to reduce the particle size from 42 nm to 45 nm. So the system temperatures are changed and the voltage value is made 800 mV to further process in high dose level at 1 KGy, 2 KGy. Considering the contending trap display by Kristianpoller et al., the supra linearity reaction was observed to be relative to the convergence of charge transporter in the two traps and radiance focuses within the vision of a solid contender. Along these lines, the decrease in the conflict at a higher portion causes additional supra linearity and more quadratic conduct [44].

IV. Conclusions

Ba_{1-x}Ca_xSO₄: Dy³⁺ phosphor was prepared by the combustion method and it is confirmed from XRD and XPS studied conducted in these materials. The outcomes demonstrate that when Dy³⁺ doped Ba_{1-x}Ca_xSO₄ is illuminated with dosages from 10 Gy to 2 KGy by utilizing Gamma chamber illumination, the supra linearity of all glow peaks increases to its f(D)_{max} at 700 Gy. From the materials the peaks 1 and 2 show second-order kinetic energy and can be utilized as the standard dosimetry peak at both low temperatures with high warming possibilities. The peaks 3 and 4 show the lower temperature area. Subsequently, it tends to be presuming that these peaks are appropriate for use in high-portion measurements, with the low temperature somewhere in the range of 10 Gy and 700 Gy. It is observed that low dose gamma-ray exposure; will be outcomes that are highly sensitive with linearity response. This is based on the materials used in the medical field in the clinical environment. To determine the estimate of presentation energy and frequency, factors were in

the range of 0.6 to 1.2 eV and 5.07±0.05x10⁶ to 3.09±0.01x10¹⁵ respectively.

V. Acknowledgement

This work is based on the research supported by the RGNF, to providing the financial support and the Department of Radiology and safety division, IGCAR, Kalpakkam for giving the opportunity to complete the radiation exposure research work.

VI. References:

- [1] Delicea S and Gasanlya N M., low temperature thermoluminescence study of GaSe: Mn layered single crystals. Taylor and Francis 2 (2016) 112-121.
- [2] Micocci G, Serra A, and Tepore A., electrical properties of n-GaSe single crystals doped with chlorine. Appl.Phys. 82 (1997) 2365-2369.
- [3] Cingolani A, Minafra P, Tantalo P, and Paorici C., Edge emission in GaSe and GaS. Phys.status solidi A 4 (1971) 83-85.
- [4] Somogyi M., Anomalous photo voltage in insulation GaSe crystals. Phys. Status Solidi A, 7 (1971) 263-267.
- [5] Mayavani A, ganesamurthi J and Gandhi S., templated synthesis and characterization of red-emitting Ca_{1-x}Sr_{1-x}Eu³⁺2x SiO₄ phosphor for LED applications. Bull.Mater.Sci. 41 (2018) 121.
- [6] Piquette A, Bergbauer W, Galler B, and Mishra K., On Choosing Phosphors for Near-UV and Blue LEDs for White Light. J. Solid State Sci. Technol., 5 (2016) 3146-3159.
- [7] Setlur A., Phosphors for LED-based Solid-State Lighting. Electro chem. Soc. Interface16 (2009) 32.
- [8] Karmes M R, Shchekin O B, Mueller G O, and Zhou L., Status and future of high power light-emitting diodes for solid-state lighting. J. Disp. Technol. 3 (2007) 160-175.
- [9] Nakamura S., Present performance of InGaN-based blue/green/yellow LEDs. Proc. SPIE. 30 (1997) 02-26.
- [10] Yan X H, Zheng S S, Yu R M, Jing C, Xu Z W, Liu C J., Preparation of YAG:Ce³⁺ phosphor by gel-gel low temperature combustion method and its luminescent properties. Trans. Nonferrous Met. Soc. China. 18 (2008) 648.

- [11] Lian S X, Lin J H, and Su M Z., the synthesis and luminescent properties of $\text{Ca}_{1-x}\text{Zn}_x\text{TiO}_3:\text{Pr}^{3+},\text{R}^+$ ($\text{R}^+=\text{Li}^+,\text{Na}^+,\text{K}^+,\text{Rb}^+,\text{Cs}^+,\text{Ag}^+$). *J. China Rare Earth Soc.*, 19 (2001) 602.
- [12] Justel T, Nikol H, and Ronda C., *New Developments in the Field of Luminescent Materials for Lighting and Displays*. Chem. Int. Ed. 37 (1998) 3084.
- [13] Liu X, Yan L, and Lin J. J., *Electro chem. Soc.*, 156 (2009) 1.
- [14] Zhu G, Ci Z, Shi Y, Que M, Wang Q, and Wang Y., Synthesis, crystal structure and luminescence characteristics of a novel red phosphor $\text{Ca}_{19}\text{Mg}_2(\text{PO}_4)_{14}:\text{Eu}^{3+}$ for light emitting diodes and field emission displays. *J.Mater. Chem. C.*, 1 (2013) 5960.
- [15] McKeever S W S. *Thermoluminescence of Solids* (Cambridge University Press) (1988).
- [16] Nameeta B, Bisen D P, Kher R S, and Khokhar M S K., Mechanoluminescence and thermoluminescence in γ -irradiated rare earth doped CaF_2 crystals. *Physics Procedia*. 2(2) (2009) 431.
- [17] Luminescence online available from <http://www.uvminerals.org/luminese.htm>.
- [18] Basuna S, Imbusch G F, Jiac D D, Yenc W M., the analysis of thermoluminescence glow curves. *J. Lumin.*, 104 (2003) 283-294.
- [19] Chen R, Kirsh Y., *Analysis of thermally stimulated processes*. Pergamon Press. 15 (1981) 167.
- [20] McKeever S W S, Moskovitch M, Townsend P D., *Thermoluminescence Dosimetry Materials: Properties and Uses*. Nuclear Technology Publishing, Ashford. (1995).
- [21] Tamrakar R K, Bisen D P., Optical and kinetic studies of $\text{CdS}:\text{Cu}$ nanoparticles, *Res. Chem. Intermed.* 38(38) (2012) 1-6.
- [22] Tamrakar R K., Thermoluminescence studies of copper doped cadmium sulphide nanoparticles with trap depth parameter. *Res. Chem. Intermed.* (2012). DOI: 10.1007/s11164-012-0940-z.
- [23] Tamrakar R.K., Thermoluminescence studies of UV-irradiated $\text{Y}_2\text{O}_3:\text{Eu}^{3+}$ doped phosphor, (2012). DOI Res Chem. Intermed. DOI: 10.1007/s11164-012-0908-z.
- [24] Tamrakar R K, Bisen D P and Brahme N., Characterization and luminescence properties of Gd_2O_3 phosphor. *Res. Chem. Intermed.*, (2013). DOI 10.1007/s11164-013-1080-9.
- [25] Chen R, McKeever S W S., *Theory of Thermoluminescence and Related Phenomena*, World Scientific. (1997) 559 pages.
- [26] Chen R, Kristianpoller N, Davidson Z, Visocekas R., Mixed first and second order kinetics in thermally stimulated processes. *Journal of Luminescence* 23(3) (1981) 293-303.
- [27] Chen R., *Methods for kinetic analysis of thermally stimulated processes*. *Journal of Materials Science*. 11(8) (1976) 1521-1541.
- [28] Fetisov A V, Kozhina G A, Estemirova S Kh, Fetisov V B, Mitrofanov V Ya, Uporov S A, and Vedmid L B., XPS Study of Mechanically Activated $\text{YBa}_2\text{Cu}_3\text{O}_{6+\delta}$ and $\text{NdBa}_2\text{Cu}_3\text{O}_{6+\delta}$. *Journal of Spectroscopy*, 13 (2013) 217-268.
- [29] Rokosz K, Hryniewicz T, Chapon P, Raen S, and Ricardo H, Sandim Z., XPS and GDOES Characterization of Porous Coating Enriched with Copper and Calcium Obtained on Tantalum via Plasma Electrolytic Oxidation. *Journal of Spectroscopy*. (2016) 7:7093071. DOI.org/10.1155/2016/7093071.
- [30] Barreca D, Gasparotto A, Milanov A, Tondello E, Devi A and Fischer A., Nanostructured Dy_2O_3 films: an XPS investigation. *Surface Science Spectra* 14 (2007) 52-59.
- [31] Chen R, McKeever S W S., *Theory of Thermoluminescence and Related Phenomena*. World Scientific, London, (1997).
- [32] May C E, Partridge J A., Thermoluminescence kinetics of alpha irradiated alkali halides. *J.Chem.Phys.* 40 (1964) 1401-1415.
- [33] Horowitz Y S, Yossian D., computerized glow curve deconvolution: application to Thermoluminescence dosimetry. *radiat.prot.dosim*, 60 (1995) 1-110.
- [34] Kongre V C, Gedam S C, Dhoble S J., Photoluminescence and Thermoluminescence characteristics of $\text{BaCa}(\text{SO}_4)_2:\text{Ce}$ mixed alkaline earth sulfate. *Journal of Luminescence*. 135 (2013) 55-59.
- [35] Michael A, Reshchikov and Hadis Morkoc., Luminescence properties of defects in GaN. *Journal of Applied Physics*. 97 (2005) 061301.
- [36] Lochab S P, Sahare P D, Chauhan R S, Numan Salah, Pandya A., Thermoluminescence of $\text{Ba}_{0.97}\text{Ca}_{0.03}\text{SO}_4:\text{Eu}$ irradiated with 48 MeV ^7Li ion beams. *J.Phys. D: Appl. Phys.* 39 (2006) 786.
- [37] Hadjipanay G C and Siegel R W., *Nanophase Materials: Synthesis, Properties, Applications*, NATO Advanced Studies Institute Kluwer, Dordrecht. (1993) 260.

- [38] Gleiter H., Nanocrystalline $Ba_{0.97}Ca_{0.03}SO_4$: Eu for ion beams dosimetry. *Prog. Mater. Sci.* 33 (1989) 223.
- [39] Lochab S P, Kanjilal D, Numan Salah, Sami Habib S, Lochab J, Ranju Ranjan, Aleynikov V E, Rupasov A A, and Pandey A., Nanocrystalline $Ba_{0.97}Ca_{0.03}SO_4$: Eu for ion beams dosimetry, *Journal of Applied Physics*. 104 (2008) 033520. DOI.org/10.1063/1.2955459
- [40] Kongre V C, Gedam S C, Dhoble S J., Thermoluminescence of gamma irradiated $BaCa(SO_4)_2$: Eu, Dy. *Radiation effects and defects solids*. 170(7) (2015) 8610-620.
- [41] Gagandeep K & Rai S B., Cool White Light Emission in Dysprosium and Salicylic Acid Doped Poly Vinyl Alcohol Film Under UV Excitation. *J Fluoresc.* 22 (2012) 475-483.
- [42] Pandey A, Sonkawade R G, Sahare P D., Thermoluminescence and photoluminescence characteristics of nanocrystalline $K_2Ca_2(SO_4)_3$: Eu. *J. Phys. D: Appl. Phys.*, 35(21) (2002) 2744-2747.
- [43] Alawiah A, Bauk S, Marashdeh M W, Ng K S, Abdul-Rashid H A, Yusoff Z, Gieszczyk W, Noramaliza M N, Mahdiraji G A, Tamchek N, Muhd-Yassin S Z, Mat-Sharif K A, Zulkifli M I, Maah M J, CheOmar S S, Bradley D A., Thermoluminescence glow curves and deconvoluted glow peaks of Ge doped flat fibers at ultra-high doses of electron radiation. *Radiation Physics and Chemistry* 113 (2015) 53–58.
- [44] Gieszczyk W, Bilski P, Olko P, Hermann R, Kettunen H, Virtanen A, Bassler N., Evaluation of the relative Thermoluminescence efficiency of LiF: Mg, Ti and LiF: Mg, Cu, P TL detectors to low-energy heavy ions. *Radiat.Meas*, 51 (2013) 7-12.